Hindawi Publishing Corporation
International Journal of Polymer Science
Volume 2015, Article ID 989516, 9 pages
http://dx.doi.org/10.1155/2015/989516

Research Article

Effect of Alginate Lyase on Biofilm-Grown *Helicobacter pylori* Probed by Atomic Force Microscopy

Alessandro Maiorana,[1] Francesca Bugli,[2] Massimiliano Papi,[1] Riccardo Torelli,[2] Gabriele Ciasca,[1] Giuseppe Maulucci,[1] Valentina Palmieri,[1] Margherita Cacaci,[2] Francesco Paroni Sterbini,[2] Brunella Posteraro,[2] Maurizio Sanguinetti,[2] and Marco De Spirito[1]

[1]*Istituto di Fisica, Università Cattolica del Sacro Cuore, Largo F. Vito 1, 00168 Roma, Italy*
[2]*Istituto di Microbiologia, Università Cattolica del Sacro Cuore, Largo F. Vito 1, 00168 Roma, Italy*

Correspondence should be addressed to Massimiliano Papi; m.papi@rm.unicatt.it

Received 8 January 2015; Revised 26 March 2015; Accepted 15 April 2015

Academic Editor: Miriam Rafailovich

Helicobacter pylori (*H. pylori*) is a microorganism with a pronounced capability of adaptation under environmental stress solicitations. Its persistence and antimicrobial resistance to the drugs commonly used in the anti-*H. pylori* therapy are associated with the development of a biofilm mainly composed of DNA, proteins, and polysaccharides. A fundamental step to increase the success of clinical treatments is the development of new strategies and molecules able to interfere with the biofilm architecture and thus able to enhance the effects of antibiotics. By using Atomic Force Microscopy and Scanning Electron Microscopy we analyzed the effects of the alginate lyase (AlgL), an enzyme able to degrade a wide class of polysaccharides, on the *H. pylori* shape, surface morphology, and biofilm adhesion properties. We demonstrated that AlgL generates a noticeable loss of *H. pylori* coccoid form in favor of the bacillary form and reduces the *H. pylori* extracellular polymeric substances (EPS).

1. Introduction

Helicobacter pylori is one of the causative agents of gastritis and peptic ulcer diseases and is also considered as a risk factor for gastric carcinoma [1, 2]. *Helicobacter pylori* is a microorganism with a pronounced capability of adaptation under environmental stress solicitations [3]. Its persistence and antimicrobial resistance to the drugs commonly used in the anti-*H. pylori* therapy are associated with genetic variability [4] and biofilm development [5–8]. *Helicobacter pylori* is capable of forming a mature biofilm characterized by clustered bacterial cells arranged in an abundant matrix after 3 days of incubation in vitro [9–11]. Although the biofilm matrix composition of *H. pylori* has not been fully elucidated, DNA, proteins, and lipids together with polysaccharides represent the most important components of the matrix extracellular polymeric substances (EPS) [12, 13].

Cell aggregation and early adhesion to surfaces are both dependent on the properties of the bacterium surface that is modulated by the composition of the extracellular matrix. The chemical structure of the biofilm along with the composition of EPS produced by the bacterium not only is critical for microbial survival in diverse environments but may facilitate survival during transmission and promote persistence in vivo [14]. *H. pylori* is able to modulate its shape from bacillary form to coccoid form to fit the environmental conditions and its virulence is strongly dependent on its cellular morphology. In general, it is regarded that the bacillary *H. pylori* transforms to the coccoid form under stressfully environmental conditions [15–18]. However, characteristics of the coccoid *H. pylori* such as the ultrastructure, the viability, or the transformation process remain largely unexplored. Transformation into the coccoid form is an active, biologically led process, switched on by the bacterium as a protection mechanism.

Transformation plays a role in the transmission of the bacteria and is thought to be partly responsible for recrudescence or relapses of infection after antimicrobial treatments.

To increase the success of clinical treatments, together with the development of new antibiotics, it is crucial to exploit molecules able to interfere with the normal biofilm architecture and able to interfere with the *H. pylori* shape [9, 19, 20]. To this purpose in this study we investigate the effect of alginate lyase (AlgL), an enzyme able to degrade some polysaccharides, on *H. pylori* biofilm formed by bacillary or coccoid shaped bacteria [21]. By using Atomic Force Microscopy (AFM) we analyzed the effects of AlgL on the *H. pylori* biofilm adhesion properties and we measured the morphological alterations of bacteria in response to the clinical treatment. AFM, among high-resolution microscopy techniques used in microbiology and diagnostics [22–25], has the capability to determine the hydrophobic/hydrophilic character of the biofilm with great sensitivity [20, 26, 27].

2. Materials and Methods

2.1. Bacterial Strains and Culture Conditions. The *H. pylori* strain used for the experiments was a clinical isolate from gastric biopsy specimens of a patient attending the Institute of Microbiology of Gemelli Hospital (Rome). Biopsy sample was cultured on Brucella agar plate containing 7% fetal calf serum (FCS), amphotericin at 5 mg/L, and vancomycin at 2 mg/L. Plate was incubated in microaerophilic atmosphere at 37°C for 3 to 5 days. Cultured bacteria were identified as *H. pylori* based on colony morphology, gram staining, and positive biochemical reactions such as urease, catalase, and oxidase. Clinical isolate, containing *vacA* and *cagA* genes as demonstrated by polymerase chain reaction, was stored at −80°C in Brucella broth supplemented with 20% glycerol and 7% FCS until experimental tests.

2.2. Biofilm Formation and Its Quantification. For the biofilm formation, bacteria were harvested in Brucella broth supplemented with 7% FCS and broth cultures were incubated overnight at 37°C in a microaerophilic atmosphere (85% N_2, 5% O_2, and 10% CO_2) under shaking at 100 rev/min.

After incubation, broth culture was adjusted to an optical density at 600 nm (A600) of 0.2 which corresponded to the beginning of exponential phase. Sterilized 13-mm-diameter glass coverslips (Bioscience Tools, San Diego, CA) were placed into a standard 24-well cell culture plate (Thermo Scientific) and each well was filled with 1 mL of the precultured cell to allowadherence of *H. pylori*. The cultures were incubated under microaerophilic conditions at 37°C for 3 days without shaking. After incubation, the coverslips were removed, washed with phosphate-buffered saline (PBS), and placed again into a clean and sterile 24-well cell culture plate. The samples were then air-dried and stained with crystal violet (CV) for 30 s. After staining, the coverslips were rinsed with distilled water to remove excess dye and then air-dried at room temperature for 30 min. For biofilm quantification, all dye associated with the biofilms was dissolved with 1 mL of 95% ethanol and 200 μL of the solutions was used to measure the absorbance at 560 nm with a microplate reader (Bio-Rad Laboratories, Hercules, CA) to determine the quantity of biofilm formation.

2.3. Alginate Lyase Treatment. The AlgL from *Flavobacterium* species (28,000 U/g) was purchased as a pure substance from Sigma-Aldrich, and a stock solution was freshly prepared in sterile PBS. We used a concentration range from 0.015 U/mL to 30 U/mL of ALgL that had previously been shown to be sufficient to reduce biofilm formation in *A. fumigatus* [20, 27]. The enzyme powder was dissolved in Brucella broth and added to the wells with mature formed biofilm. Plate was incubated under microaerophilic conditions at 37°C for 16 h. A growth control well was incubated with only Brucella broth.

2.4. Atomic Force Microscopy. A Nanowizard II atomic force microscope (JPK Instruments AG, Berlin, Germany) mounted on an optical microscope (Axio Observer Carl Zeiss, Oberkochen, Germany) was used for imaging each sample. The images were acquired using silicon cantilevers with high aspect-ratio conical silicon tips (CSC16 Mikro-Masch, Tallinn, Estonia) characterized by an end radius of about 10 nm and a half conical angle of 20°. All these cantilevers, with a nominal spring constant of about $k = 0.01$ N/m, were accurately calibrated as previously reported [28, 29]. All images were acquired at 512 × 512 pixels and processed by means of Gwyddion software. A large scan area (50 × 50 μm) was imaged in order to determine the shape of the bacterium (coccoid or bacillary). In particular, the method used for cellular morphology quantification, bacillary or coccoid, involved a measurement of circularity directly from 10 different AFM images for each sample by using ImageJ software. The value of circularity is calculated as $4\pi * \text{area}/\text{perimeter}^2$. A value of 1.0 indicates a perfect circle. As the value approaches 0.0, it indicates an increasingly elongated shape.

To characterize the surface properties of *H. pylori* biofilm we calculated the Root Mean Square Roughness (RMS) directly from 10 different AFM images for each sample by using Gwyddion software. RMS is the root mean square of the vertical distance r_i from the mean line to the ith data point:

$$\text{RMS} = \sqrt{\frac{1}{N}\sum_{j=1}^{N} r_j^2}. \quad (1)$$

For each sample a histogram of RMS values was calculated by using 20 different images and calculating the RMS values in different areas. Each histogram was fitted by Gaussian functions by using OriginPro software. All experiments were performed in air at room temperature (~25°C) with a measured average relative humidity of 75%.

2.5. Adhesion Force Spectroscopy. Adhesion force spectroscopy maps were done by recording matrix of 25 × 25 force-distance curves on areas by using different magnifications. The force applied on the samples was set to 1.5 nN in all force spectroscopy points. All the force versus distance curves were obtained using the same force set point and keeping a constant speed of 1.0 μm/s; the total vertical

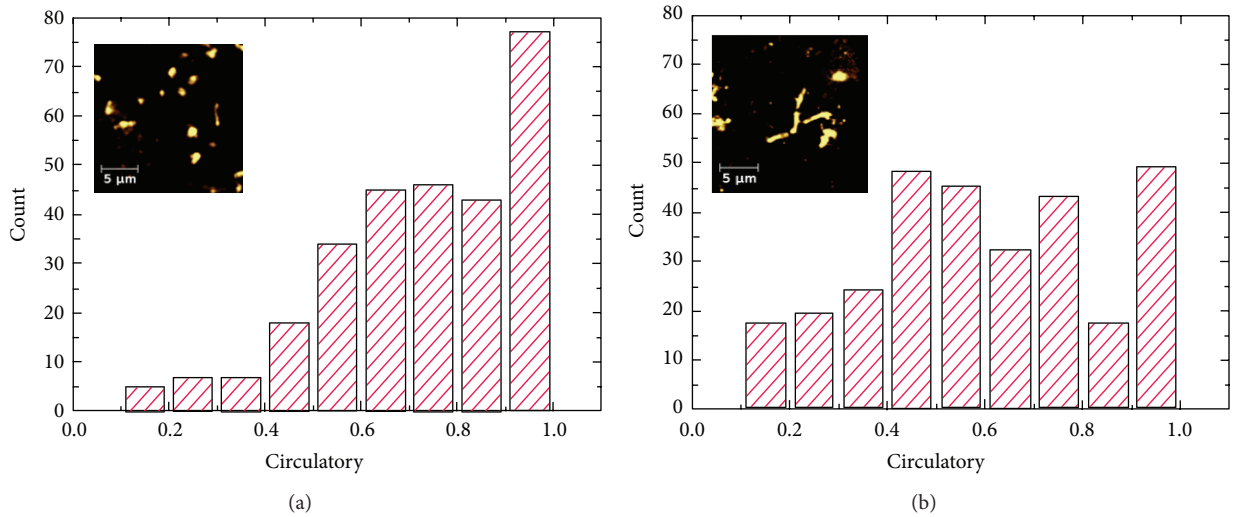

Figure 1: Quantitative (a-b) analysis of *H. pylori* biofilm cell morphologies in (c-d) circularity distribution is shown for each sample. The distribution was calculated by means of ten different AFM images for each sample and following the measuring system described in Section 2. Inset images show representative AFM images ($20 \times 20\ \mu$m) for each sample, which highlights the different shapes.

displacement was set to 1.0 μm. Force-distance curves were analysed using the data processing supplied with the JPK Nanowizard II AFM system. In brief, deflection data were recorded during the retraction of the tip from the biofilm surface and converted to force after multiplication with the spring constant of cantilever, whereas the real tip-substrate distance was obtained by subtracting the deflection value from the piezo movement. The point of zero distance was assigned at the intersection of the experimental curve with the straight line fitting the tail of the curve. Adhesion values were deduced from the force versus distance curves as the maximum value in the retraction curve [30]. For each sample a histogram of adhesion values was calculated by using 5 different maps and was fitted by Gaussian functions. All experiments were performed in air at room temperature (~25°C) and at average relative humidity of 75%.

2.6. Scanning Electron Microscopy. For SEM imaging, samples on coverslips were processed as explained before [31]. Briefly, samples were washed three times with 0.1 M sodium cacodylate buffer (pH 7.4) and then dehydrated serially in 30%, 50%, 70%, 90%, and 100% ethanol. Finally samples were fixed for 1 hour with 2% osmium tetra-oxide (OsO4). The SEM procedures were completed by drying the samples and sputtering 8 nm gold layer. Micrographs were collected with a Zeiss Supra 25 microscope (Germany).

3. Results

The clinical strain of *H. pylori* used in our study was demonstrated to be a high biofilm producer by crystal violet staining (data not shown). In the inset of Figure 1 two representative AFM topological images of the *H. pylori* before (Figure 1(a)) and after (Figure 1(b)) the treatment with 30 U/mL of AlgL are reported. It appears that the AlgL treatment deeply modifies the *bacterium* shape inducing a noticeable loss of the coccoid rounded form in favour of the more elongated bacillary form. This result is further confirmed by the circularity distributions obtained before (Figure 1(a)) and after (Figure 1(b)) the AlgL treatment. Distributions were calculated as described in Materials and Methods by means of ten different AFM images for each sample. The two distributions appear to be very spread out since *H. pylori* assumes a large *ensemble* of coexisting conformations in both cases.

However, the interaction of the 30 U/mL AlgL with the biofilm has a significant effect on the distribution shape inducing a decrease of its mean value from ~0.78 down to a value of ~0.63. This decrease clearly reflects a higher statistical occurrence of the more elongated conformations instead of the more compacted ones.

In Figures 2(a) and 2(b) two representative topological images showing bacteria enveloped in the EPS before and after the 30 U/mL AlgL treatment are reported. In Figure 2(e) several features resembling fractures (see white arrow) are clearly visible within the EPS surface. This finding demonstrates that, together with the direct effect of the AlgL on the *H. pylori* shape, the enzyme produces a significant alteration in the biofilm architecture forming fractures in the EPS matrix that envelope the bacteria. In Figures 2(b) and 2(c) the relative deflection images of the same two samples before and after the AlgL treatment highlight the structural EPS differences and the loss of homogeneity produced by the enzymatic activity.

To quantify the structural modification in the EPS structure we computed the biofilm surface roughness (RMS) by using (1) from ten different topological images obtained from 3 independent samples. The biofilm RMS distributions acquired before and after the AlgL treatment are shown in Figures 2(g) and 2(h), respectively. A Gaussian analysis has been performed on both distributions. The biofilm RMS distribution before the AlgL treatment shows a Gaussian shape peaked at 26 nm (see histogram in Figure 2(g)) whereas

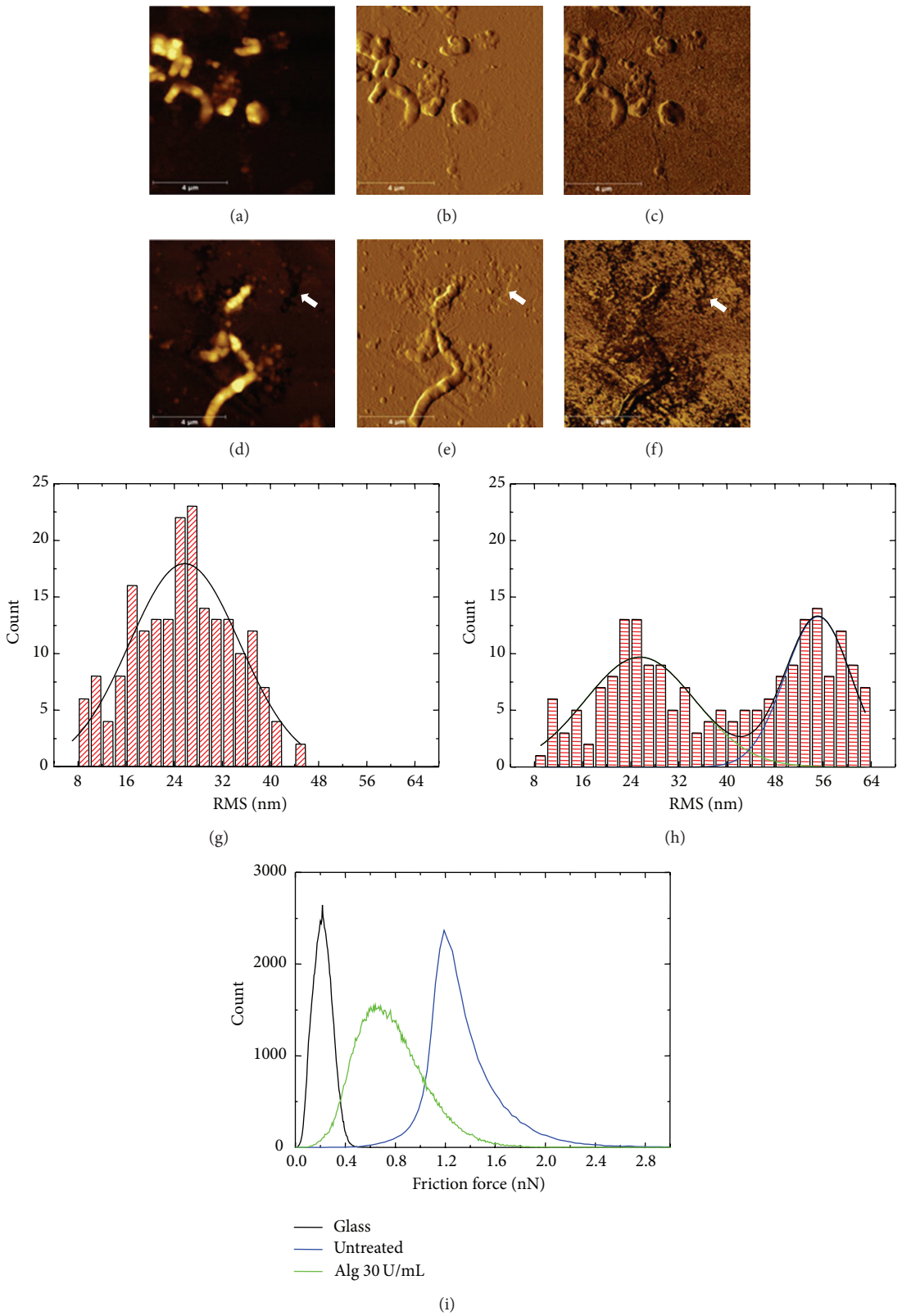

Figure 2: Representative zoom AFM images (10 × 10 μm) of *H. pylori* biofilm are shown before treatment (a–c) and after treatment with AlgL (e–g). Height images (a and d) show different cells from each experimental condition and the presence of fractures in biofilm generated by AlgL treatment (d). Deflection and lateral images (b, e, c and f) reveal more details in biofilm texture. In Figures (g and h) the roughness distribution and Gaussian fit (black lines) are shown for each sample. The distributions were obtained following the procedure described in Section 2. Distributions of the friction forces between AFM tip and three different surfaces: clean glass, biofilm, and biofilm treated with 30 U/mL AlgL (i).

after the AlgL treatment the distribution is much more spread encompassing two different peaks at ~26 nm and ~55 nm (see histogram in Figure 2(h)). The occurrence of two peaks reflects the presence of two morphologically different regions in the EPS matrix. The first peak at ~26 nm rises from all those samples areas not affected by the enzymatic EPS digestion whereas the second peak at ~55 nm rises from the areas where the EPS layer is dramatically reduced showing fractures of different sizes, from few nanometres up to several microns. In Figures 2(c) and 2(f) the relative torsional images, produced by the torsion of the AFM cantilever, obtained from the two samples before and after the AlgL treatment, are also reported. Torsional images are able to quantify the friction forces between the sample surface and the AFM silicon tip. In Figure 2(c) the friction force shows a homogeneous value all over the EPS surface whereas in Figure 2(f) the friction forces significantly change inside and outside the fractures. In Figure 2(i) three different friction force distributions are reported. The average friction force between the AFM tip and the biofilm decreases from a value of ~1.2 nN to 0.5 nN after the AlgL treatment and several areas of the sample showed a value of about 0.2 nN, a value very similar to the friction force between the cantilever tip and the clean glass coverslip. These results clearly evidence a difference in the holes surface chemical properties due to the contact of the AFM tip with the glass coverslip under the EPS.

A direct evaluation of the biofilm chemical properties can be achieved by mapping the adhesion properties of the biofilm surface by atomic force spectroscopy. In Figures 3(a) and 3(d) two representative magnifications of a *H. pylori* bacterium surrounded by EPS before and after the AlgL treatment are shown and in Figures 3(b) and 3(f) the corresponding adhesion maps (25 × 25 pixels) with the bacteria perimeter highlighted in red are reported. The same colour scale has been used in both cases. By comparing the two maps, a huge increase of biofilm adhesion can be clearly detected after the AlgL treatment. This increase is mainly located in the region outside the bacterium, whereas the increase in the region occupied by the bacterium appears to be less pronounced.

A more quantitative comparison between the EPS adhesion properties before and after the AlgL treatment is shown in Figures 3(c) and 3(e), where the statistical distribution of the adhesion values is reported for both cases. Before the AlgL treatment, the biofilm adhesion displays a bell shaped distribution with adhesion values ranging between 0 nN and 21 nN and with a peak value of about ~ 6nN (see histogram in Figure 3(c)). In this condition, the *H. pylori* biofilm has a hydrophobic behaviour along the whole sample even if it is slightly more hydrophobic outside the bacteria. Conversely, after the AlgL treatment a wider distribution can be detected with adhesion values up to 30 nN. A Gaussian analysis of the distribution highlights the presence of tree peaks approximately positioned at 8 nN, 18 nN, and 27 nN. The wider adhesion values distribution and the occurrence of three distinct peaks highlight once again that the AlgL treatment induces deep structural modifications in the EPS matrix. In this regard, worthy of note is the arising of a third peak centred at 27 nN. This peak encompasses value ranging between 24 and 30 nN that are consistent with the measured adhesion value of the silica tip with the bare glass coverslip (~29 nN) [28, 29]. This result clearly confirms that, aside from the modification of the bacterium shape, the AlgL treatment induces the formation of nano- and microfractures of the EPS matrix and therefore can be highly effective in the disruption of the bacterial biofilm.

In Figure 4(b) the effect of five different concentrations of AlgL on the *H. pylori* biofilm structure is reported. As the enzyme concentration increases, the cell circularity decreases and the surface of fractured EPS increases showing a clear dose-dependent enzymatic effect of the AlgL on the *H. pylori* biofilm. Only for the lower concentration, AlgL = 0.015 U/mL, we did not observe any difference between the treated and the untreated samples. When the AlgL has a concentration of 0.15 u/mL some biofilm fractures and several elongated cells are observable (see Figure 4(a)). At 30 U/mL almost half of the surface is clearly lysed and the *H. pylori* bacillary form becomes predominant (see Figure 4(c)).

4. Discussion

Helicobacter pylori is a bacillary shaped Gram negative bacterium, which colonizes the gastric mucosa where pH falls to ~1.5 in the absence of food and to ~5.0 during the digestive phase [1]. *H. pylori* infection has an estimated prevalence of about half the world's population [32], making this pathogen one of the most successful human pathogens. Infection by this bacterium has been associated with increased risk for the development of gastritis, peptic ulcer disease, and gastric adenocarcinomas [33, 34]. Similar to other microorganisms, *H. pylori* is able to form biofilm structure which has been observed in vitro at air/liquid interfaces in media with a high carbon/nitrogen ratio [35]. Even if the significance of biofilm in pathogenesis of *H. pylori* infections is not yet fully understood, to increase the success of clinical treatments, the development of new strategies able to interfere with the biofilm architecture and thus able to enhance the effects of antibiotics is fundamental. In this work we analyzed the effects of the alginate lyase on the *H. pylori* shape, surface morphology, and biofilm adhesion properties. We demonstrated that AlgL generates a noticeable loss of *H. pylori* coccoid form in favour of the bacillary form and reduces the *H. pylori* extracellular polymeric substances (EPS). *H. pylori* is morphologically divided into two types: a bacillary and a coccoid form [3]. The bacillary forms are viable and culturable in vitro, while the coccoid forms are viable and less culturable [36].

It is well known that the helical forms of *H. pylori* are transformed into coccoid forms as a result of many factors, like ageing and stress conditions such as starvation or the presence of antibiotics. Reversion from the coccoid state to the bacillary form, although less frequent, was however highlighted in some studies [37]. Coccoid form of *H. pylori*, initially considered quiescent bacterium, retains an essential role in relapse and gastritis complications and is capable of reverting to the bacillary state [38, 39]. In our data, AlgL activity resulted in a response of *H. pylori* in terms of morphology change. A possible explanation could be that

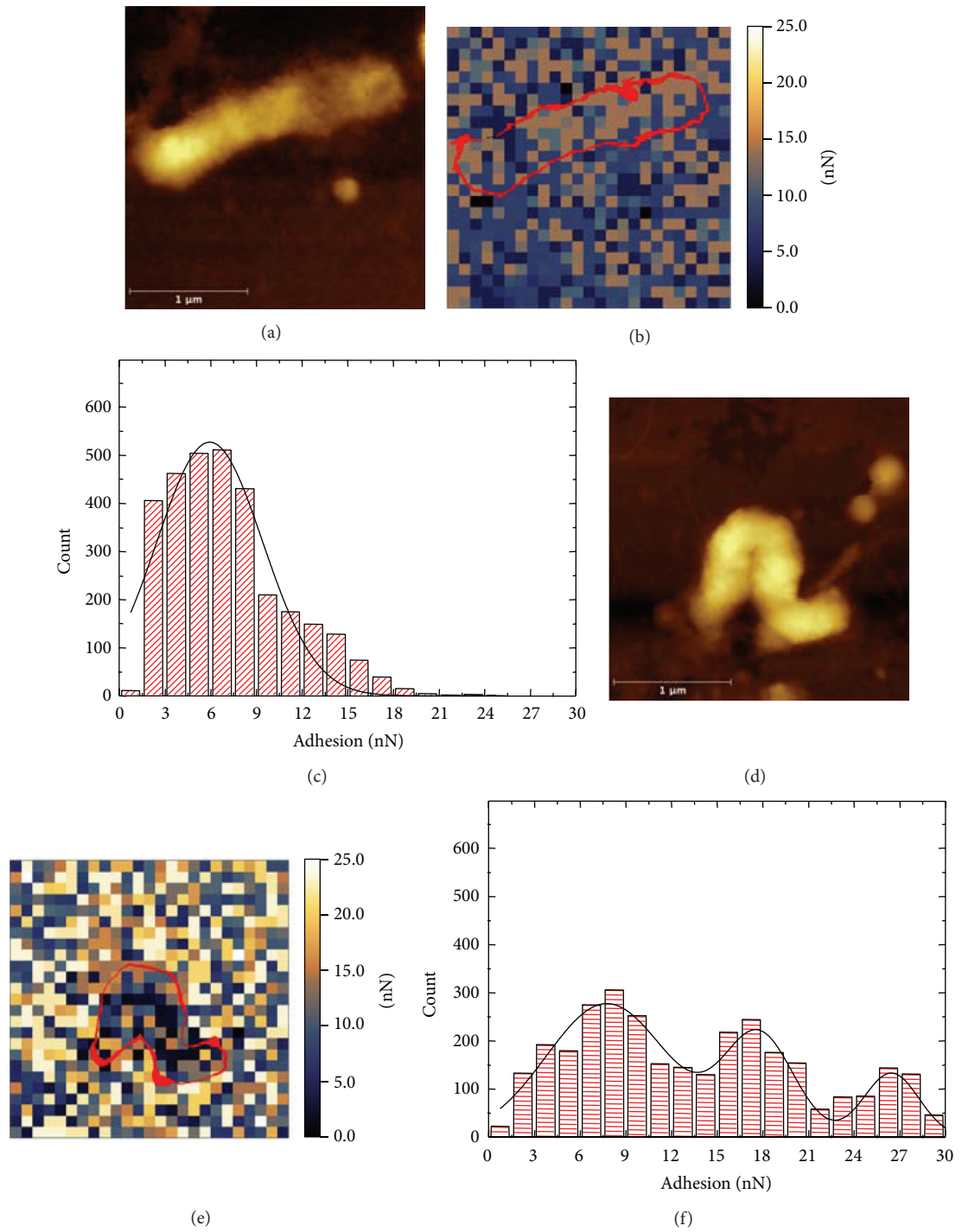

FIGURE 3: Adhesion force maps of *H. pylori* biofilm: (a) representative high-resolution image (2.3 × 2.3 μm) of *H. pylori* before treatment (a) and after treatment with AlgL (d). Representative adhesion force maps (25 × 25 pixels) with shadows of bacteria (red lines) were shown for *H. pylori* before treatment (b) and after treatment with AlgL (e). Histograms and Gaussian fit (black lines) obtained from five different maps for *H. pylori* before treatment (c) and after treatment with AlgL (f).

the enzyme does not lead to a stress condition for the bacteria but its effect on the EPS's polysaccharides could promote, in response to the well-known quorum sensing signalling, the bacillary form morphology able to actively produce EPS and leave the biofilm community as planktonic bacterium. Production of biofilm by *H. pylori* has important effect in promoting its resistance to antimicrobials and host defense factors [40]. It is generally accepted that the *H. pylori* dormant states of coccoid forms can survive for a long time in the gastric environment. Coccoid forms are metabolically quiescent

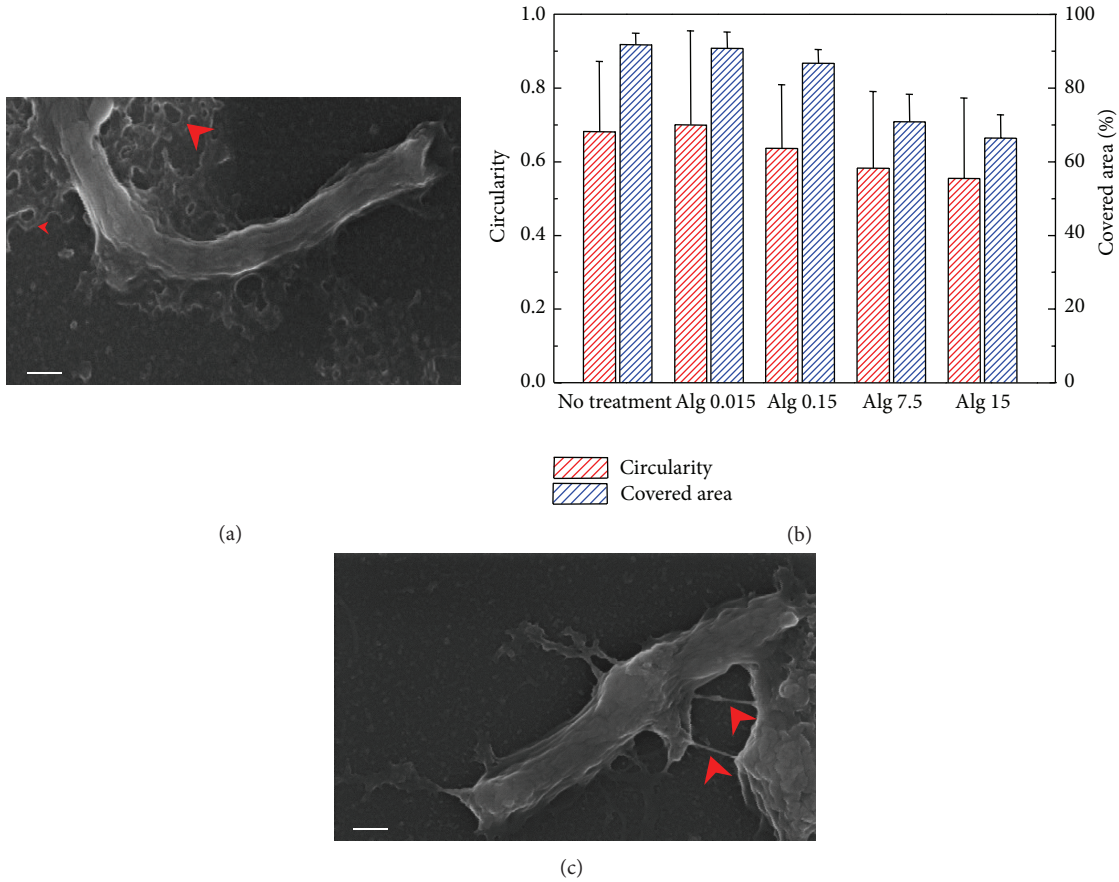

FIGURE 4: *H. pylori* circularity and percentage of surface covered by the biofilm for 5 different concentrations of AlgL (0.015, 0.15, 7.5, 15, and 39 U/mL) (b). Representative SEM images of *H. pylori* biofilm after the treatment with 0.15 U/mL of AlgL (a) and with 30 U/mL of AlgL. (c) Red arrows show the lysed EPS produced by the *H. pylori*. Scale bar 400 nm.

and have been shown, in some cases, to become selectively resistant to antibiotics. These forms probably contribute to the therapeutic failure and relapses of infections. Treatment with AlgL seems to prevent the transformation to coccoid forms retaining most of the bacteria in the spiral shape, hence creating a favourable condition to future combined treatment with antibacterial drugs [19, 41].

Treatments with standard antibiotics are often ineffective at eradicating biofilm-related infections. Because the role of *H. pylori* extracellular matrix in delaying the penetration of the drugs in the colony is still unknown; the best antibacterial drug should not be selected only on the basis of its efficiency to kill in vitro grown bacteria but also on its ability to penetrate EPS.

In this work, to study the permeability properties of an EPS reconstituted in vitro that mimics the in vivo EPS, we used AFM, which is an excellent method for the determination of the hydrophobic/hydrophilic character of the biofilm with great sensitivity [20, 26, 27].

We demonstrated that the presence of AlgL can greatly reduce the extent of the *H. pylori* biofilm forming several nano- and microfractures, which can allow the drugs transit and thus enhance their effect on the cell walls. Finally, since to devise novel and efficient pharmacological strategies based on the synergistic activity of drugs and AlgL a spatial and temporal detailed knowledge of the AlgL ability to break up and disrupt the biofilm structures is fundamental, AFM can be applied to evaluate the "in vitro" effects of a specific treatment on adhesions or other physical aspects that are crucial for the establishment and persistence of microbial biofilm.

Conflict of Interests

The authors declare that there is no conflict of interests regarding the publication of this paper.

Authors' Contribution

Alessandro Maiorana and Francesca Bugli contributed equally to this work.

References

[1] S. Suerbaum and P. Michetti, "*Helicobacter pylori* infection," *The New England Journal of Medicine*, vol. 347, no. 15, pp. 1175–1186, 2002.

[2] T. Watanabe, M. Tada, H. Nagi, S. Sasaki, and M. Nakao, "*Helicobacter pylori* infection induces gastric cancer in Mongolian gerbils," *Gastroenterology*, vol. 115, no. 3, pp. 642–648, 1998.

[3] L. P. Andersen and L. Rasmussen, "*Helicobacter pylori*—coccoid forms and biofilm formation," *FEMS Immunology and Medical Microbiology*, vol. 56, no. 2, pp. 112–115, 2009.

[4] L. Cellini, R. Grande, E. di Campli, S. di Bartolomeo, S. Capodicasa, and L. Marzio, "Analysis of genetic variability, antimicrobial susceptibility and virulence markers in *Helicobacter pylori* identified in Central Italy," *Scandinavian Journal of Gastroenterology*, vol. 41, no. 3, pp. 280–287, 2006.

[5] M. A. Carron, V. R. Tran, C. Sugawa, and J. M. Coticchia, "Identification of *Helicobacter pylori* biofilms in human gastric mucosa," *Journal of Gastrointestinal Surgery*, vol. 10, no. 5, pp. 712–717, 2006.

[6] L. Cellini, R. Grande, T. Traini et al., "Biofilm formation and modulation of luxS and rpoD expression by *Helicobacter pylori*," *Biofilms*, vol. 2, no. 2, pp. 119–127, 2005.

[7] S. P. Cole, J. Harwood, R. Lee, R. She, and D. G. Guiney, "Characterization of monospecies biofilm formation by *Helicobacter pylori*," *Journal of Bacteriology*, vol. 186, no. 10, pp. 3124–3132, 2004.

[8] J. M. Coticchia, C. Sugawa, V. R. Tran, J. Gurrola, E. Kowalski, and M. A. Carron, "Presence and density of *Helicobacter pylori* biofilms in human gastric mucosa in patients with peptic ulcer disease," *Journal of Gastrointestinal Surgery*, vol. 10, no. 6, pp. 883–889, 2006.

[9] G. Cammarota, M. Sanguinetti, A. Gallo, and B. Posteraro, "Review article: biofilm formation by *Helicobacter pylori* as a target for eradication of resistant infection," *Alimentary Pharmacology and Therapeutics*, vol. 36, no. 3, pp. 222–230, 2012.

[10] F.-L. Yang, A. M. Hassanbhai, H.-Y. Chen et al., "Proteomannans in Biofilm of *Helicobacter pylori* ATCC 43504," *Helicobacter*, vol. 16, no. 2, pp. 89–98, 2011.

[11] H. Yonezawa, T. Osaki, S. Kurata et al., "Outer membrane vesicles of helicobacter pylori TK1402 are involved in biofilm formation," *BMC Microbiology*, vol. 9, article 197, 2009.

[12] R. Grande, M. Di Giulio, L. J. Bessa et al., "Extracellular DNA in *Helicobacter pylori* biofilm: a backstairs rumour," *Journal of Applied Microbiology*, vol. 110, no. 2, pp. 490–498, 2011.

[13] R. M. Stark, G. J. Gerwig, R. S. Pitman et al., "Biofilm formation by *Helicobacter pylori*," *Letters in Applied Microbiology*, vol. 28, no. 2, pp. 121–126, 1999.

[14] L. J. Bessa, R. Grande, D. D. Iorio, M. D. Giulio, E. D. Campli, and L. Cellini, "*Helicobacter pylori* free-living and biofilm modes of growth: behavior in response to different culture media," *APMIS*, vol. 121, no. 6, pp. 549–560, 2013.

[15] M. Benaïssa, P. Babin, N. Quellard, L. Pezennec, Y. Cenatiempo, and J. L. Fauchère, "Changes in *Helicobacter pylori* ultrastructure and antigens during conversion from the bacillary to the coccoid form," *Infection and Immunity*, vol. 64, no. 6, pp. 2331–2335, 1996.

[16] J. Hua and B. Ho, "Is the coccoid form of *Helicobacter pylori* viable?" *Microbios*, vol. 87, no. 351, pp. 103–112, 1996.

[17] N. Saito, K. Konishi, F. Sato et al., "Plural transformation-processes from bacillary to coccoid Helicobacter pylori and its viability," *Journal of Infection*, vol. 46, pp. 49–55, 2003.

[18] F. Sato, "*Helicobacter pylori* in culture: an ultrastructural study," *Hokkaido Journal of Medical Science*, vol. 75, no. 3, pp. 187–196, 2000.

[19] V. Berry, K. Jennings, and G. Woodnutt, "Bactericidal and morphological effects of amoxicillin on *Helicobacter pylori*," *Antimicrobial Agents and Chemotherapy*, vol. 39, no. 8, pp. 1859–1861, 1995.

[20] F. Bugli, B. Posteraro, M. Papi et al., "*In vitro* interaction between alginate lyase and amphotericin B against *Aspergillus fumigatus* biofilm determined by different methods," *Antimicrobial Agents and Chemotherapy*, vol. 57, no. 3, pp. 1275–1282, 2013.

[21] J. W. Lampp and K. E. Griswold, "Alginate lyase exhibits catalysis-independent biofilm dispersion and antibiotic synergy," *Antimicrobial Agents and Chemotherapy*, vol. 57, no. 1, pp. 137–145, 2013.

[22] M. Papi, G. Arcovito, M. De Spirito, M. Vassalli, and B. Tiribilli, "Fluid viscosity determination by means of uncalibrated atomic force microscopy cantilevers," *Applied Physics Letters*, vol. 88, no. 19, Article ID 194102, 2006.

[23] A. Boccaccio, L. Lamberti, M. Papi et al., "A hybrid characterization framework to determine the visco-hyperelastic properties of a porcine zona pellucid," *Interface Focus*, vol. 4, no. 2, Article ID 20130066, 2014.

[24] S. K. Garg, E. Valente, E. Greco et al., "Lysophosphatidic acid enhances antimycobacterial activity both in vitro and ex vivo," *Clinical Immunology*, vol. 121, no. 1, pp. 23–28, 2006.

[25] E. Greco, M. B. Santucci, M. Sali et al., "Natural lysophospholipids reduce *Mycobacterium tuberculosis*-induced cytotoxicity and induce anti-mycobacterial activity by a phagolysosome maturation-dependent mechanism in A549 type II alveolar epithelial cells," *Immunology*, vol. 129, no. 1, pp. 125–132, 2010.

[26] G. L. Scaglione, S. Lancellotti, M. Papi et al., "The type 2B p.R1306W natural mutation of von Willebrand factor dramatically enhances the multimer sensitivity to shear stress," *Journal of Thrombosis and Haemostasis*, vol. 11, no. 9, pp. 1688–1698, 2013.

[27] A. Maiorana, M. Papi, F. Bugli et al., "A fast and quantitative evaluation of the Aspergillus fumigatus biofilm adhesion properties by means of digital pulsed force mode," *Applied Surface Science*, vol. 279, pp. 409–415, 2013.

[28] A. Boccaccio, M. Papi, M. De Spirito, L. Lamberti, and C. Pappalettere, "Effect of the residual stress on soft sample nanoindentation," *Applied Physics Letters*, vol. 102, no. 13, Article ID 133704, 2013.

[29] M. Papi, A. Maiorana, F. Bugli et al., "Detection of biofilm-grown *Aspergillus fumigatus* by means of atomic force spectroscopy: ultrastructural effects of alginate lyase," *Microscopy and Microanalysis*, vol. 18, no. 5, pp. 1088–1094, 2012.

[30] M. Papi, P. Paoletti, B. Geraghty, and R. Akhtar, "Nanoscale characterization of the biomechanical properties of collagen fibrils in the sclera," *Applied Physics Letters*, vol. 104, Article ID 103703, 2014.

[31] V. Palmieri, D. Lucchetti, A. Maiorana et al., "Biomechanical investigation of colorectal cancer cells," *Applied Physics Letters*, vol. 105, Article ID 123701, 2014.

[32] A. Covacci, J. L. Telford, G. Del Giudice, J. Parsonnet, and R. Rappuoli, "*Helicobacter pylori* virulence and genetic geography," *Science*, vol. 284, no. 5418, pp. 1328–1333, 1999.

[33] R. M. Peek Jr. and M. J. Blaser, "*Helicobacter pylori* and gastrointestinal tract adenocarcinomas," *Nature Reviews Cancer*, vol. 2, no. 1, pp. 28–37, 2002.

[34] Y. Yamaoka and D. Y. Graham, "*Helicobacter pylori* virulence and cancer pathogenesis," *Future Oncology*, vol. 10, pp. 1487–1500, 2014.

[35] L. Cellini, R. Grande, E. di Campli et al., "Characterization of an *Helicobacter pylori* environmental strain," *Journal of Applied Microbiology*, vol. 105, no. 3, pp. 761–769, 2008.

[36] H. Zeng, G. Guo, X. H. Mao, W. de Tong, and Q. M. Zou, "Proteomic insights into *Helicobacter pylori* coccoid forms under oxidative stress," *Current Microbiology*, vol. 57, no. 4, pp. 281–286, 2008.

[37] M. I. Brenciaglia, A. M. Fornara, M. M. Scaltrito, and F. Dubini, "*Helicobacter pylori*: cultivability and antibiotic susceptibility of coccoid forms," *International Journal of Antimicrobial Agents*, vol. 13, no. 4, pp. 237–241, 2000.

[38] N. Li, L. Han, J. Chen, X. Lin, H. Chen, and F. She, "Proliferative and apoptotic effects of gastric epithelial cells induced by coccoid *Helicobacter pylori*," *Journal of Basic Microbiology*, vol. 53, no. 2, pp. 147–155, 2013.

[39] F. Poursina, J. Faghri, S. Moghim et al., "Assessment of cagE and babA mRNA expression during morphological conversion of *Helicobacter pylori* from spiral to coccoid," *Current Microbiology*, vol. 66, no. 4, pp. 406–413, 2013.

[40] M. H. M. G. Houben, D. van de Beek, E. F. Hensen, A. J. M. de Craen, E. A. J. Rauws, and G. N. J. Tytgat, "A systematic review of *Helicobacter pylori* eradication therapy—the impact of antimicrobial resistance on eradication rates," *Alimentary Pharmacology and Therapeutics*, vol. 13, no. 8, pp. 1047–1055, 1999.

[41] J. Faghri, F. Poursina, S. Moghim et al., "Morphological and bactericidal effects of different antibiotics on *Helicobacter pylori*," *Jundishapur Journal of Microbiology*, vol. 7, no. 1, Article ID e8704, 2014.